nature immunology

Human uracil–DNA glycosylase deficiency associated with profoundly impaired immunoglobulin class-switch recombination

Kohsuke Imai[1], Geir Slupphaug[2], Wen-I Lee[3,4], Patrick Revy[1], Shigeaki Nonoyama[5], Nadia Catalan[1], Leman Yel[6], Monique Forveille[1], Bodil Kavli[2], Hans E Krokan[2], Hans D Ochs[3], Alain Fischer[1,7] & Anne Durandy[1]

Activation-induced cytidine deaminase (AID) is a 'master molecule' in immunoglobulin (Ig) class-switch recombination (CSR) and somatic hypermutation (SHM) generation, AID deficiencies are associated with hyper-IgM phenotypes in humans and mice. We show here that recessive mutations of the gene encoding uracil–DNA glycosylase (*UNG*) are associated with profound impairment in CSR at a DNA precleavage step and with a partial disturbance of the SHM pattern in three patients with hyper-IgM syndrome. Together with the finding that nuclear *UNG* expression was induced in activated B cells, these data support a model of CSR and SHM in which AID deaminates cytosine into uracil in targeted DNA (immunoglobulin switch or variable regions), followed by uracil removal by UNG.

Antigen-dependent immunoglobulin gene alterations such as CSR and SHM are key events in the adaptation of the B cell response through the modification of effector function and affinity to antigen, respectively. CSR and SHM processes share common steps: chromatin opening of the target regions (immunoglobulin switch (S) and variable (V) regions, respectively) associated with transcription, followed by DNA cleavage, repair and ligation[1,2]. The CSR process is initiated by chromatin opening in S regions located 5′ of the constant (C) region and mediated by cytokine-inducible germline transcription from the intron (I) promoter located 5′ of the S regions. Thereafter, the intervening DNA between the two S regions is excised and the functional transcripts (V_H-C_x) are produced after the recombination process[3].

Further understanding of these pathways at a molecular level has been provided by gene identification in part related to the analysis of a primary immunodeficiency condition, the hyper-IgM syndrome (HIGM). HIGM is characterized by normal or increased serum IgM concentrations associated with low or absent serum IgG, IgA and IgE concentrations, indicating a defect in the CSR process[4]. HIGM is a heterogeneous condition, as several molecular defects result in this syndrome. Deficiencies in CD40L (HIGM1)[5–8] and CD40 (HIGM3)[9] result in impaired T cell–B cell cooperation, leading to defective germinal center formation and impaired CSR. In another HIGM condition (HIGM2), a B cell–specific CSR deficiency has been associated with mutations in *AICDA*, the gene encoding AID[10], which is selectively expressed in B cells from germinal centers[11]. The AID defect leads not only to profoundly impaired CSR but also to defective generation of SHM in the V region of immunoglobulin genes[10]. An identical phenotype has been found in AID-deficient mice[12]. Strong evidence has been provided for involvement of AID in the generation of DNA breaks necessary for both CSR and SHM after germline transcription of the target genes[13,14]. However, its mechanism of action remains controversial. AID was originally proposed to act as an RNA-editing enzyme because of its sequence similarity to APOBEC-1, a cytidine deaminase with well known RNA-editing activity[12]. According to this proposal, endonuclease-encoding RNA would be the potential substrate of AID. However, evidence for DNA-editing activity for AID was provided by an increased frequency of consistent transition mutations in dG-dC pairs in *Escherichia coli* expressing human AID[15]. Moreover, it was demonstrated that *in vitro* AID deaminates cytosine to uracil in single-stranded DNA[16–18]. In addition, indirect evidence for involvement of AID in deamination of cytosine residues has been provided by the description of the immunological abnormalities found in UNG-deficient mice, which are characterized by partially defective CSR and a biased pattern of somatic hypermutation toward transitions at dG-dC nucleotides[19]. The phenotype of UNG-deficient mice could be explained by the defective removal from DNA of the uracil residues generated by the deamination of cytosine residues by AID. We show here that UNG deficiency in humans leads to very profound impairment of CSR and a biased pattern of SHM, demonstrating

[1]Institut National de la Santé et de la Recherche Médicale Unité 429, Hôpital Necker-Enfants Malades, 75015 Paris, France. [2]Department of Cancer Research and Molecular Medicine, Norwegian University of Science and Technology, N-7489 Trondheim, Norway. [3]Department of Pediatrics, University of Washington, Seattle, Washington 98195-6320, USA. [4]Department of Pediatrics, Chang Gung Children's Hospital and University, 333, Taoyuan, Taiwan, China. [5]Department of Pediatrics, National Defense Medical College, 359-8513, Saitama, Japan. [6]Division of Basic and Clinical Immunology, Department of Medicine, University of California, Irvine, California 92697, USA. [7]Unité d'Immunologie-Hématologie et Rhumatologie Pédiatrique, Hôpital Necker-Enfants Malades, 75015 Paris, France. Correspondence should be addressed to A.D. (durandy@necker.fr).

Published online 7 September 2003; doi:10.1038/ni974

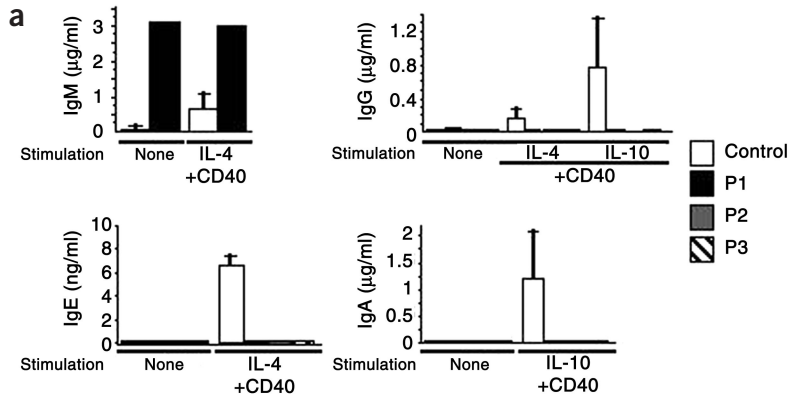

Figure 1 Defective CSR in patients at a precleavage step. (**a**) Impaired *in vitro* CSR in B cells from patients. PBMCs were activated for 12 d in presence of CD40 monoclonal antibody or soluble CD40L plus IL-4 or IL-10. Immunoglobulin production was assessed by enzyme-linked immunosorbent assay. (**b**) Defective expression of IgE circle and functional transcripts in patient B cells. PBMCs were activated for 5 d with soluble CD40L (sCD40L) plus IL-4, and transcripts of genes encoding CD19, AICDA and IgE were detected by RT-PCR. GLT (I_ε-C_ε), germline transcripts; CT (C_μ-I_ε), circle transcripts; FT (V_H-C_ε), functional transcripts. (**c**) Defective CSR-associated DNA double-strand breaks occurrence in Sμ regions in B cells from patients. Viable B cells ($CD19^+$, propidium iodide–negative) from controls (C1–C6), P1 and P3 were purified after 5 d of activation with soluble CD40L plus IL-4. Ligation-mediated PCR products were hybridized with a radiolabeled Sμ probe (exposure time, 18 h). Hybridization revealed several bands in activated B cells from the six controls (two independent results were shown for C5 and C6). T cells activated by anti-CD3 plus IL-2 were used as a negative control. Experiments were done three times for P1 and twice for P3 with same negative results. Ligation-mediated PCR products from controls were cloned and sequenced, and show actual ligation of the linker to Sμ regions at different sites in 56% of clones.

that UNG is essential in this process and supporting the DNA-editing model of AID.

RESULTS

Characterization of molecular defects in *UNG*$^{-/-}$ humans

We studied three unrelated patients (P1, P2 and P3) affected with HIGM, which has characteristics very similar to those of AID deficiency (HIGM2), including susceptibility to bacterial infections, lymphoid hyperplasia, increased serum IgM concentrations and profoundly decreased serum IgG and IgA concentrations (**Table 1**). B cells from these patients were unable to undergo CSR *in vitro* after activation with antibody to CD40 (anti-CD40) or with soluble CD40 ligand (CD40L) plus interleukin 4 (IL-4) or IL-10 (**Fig. 1a**). IgG, IgA and IgE molecules as well as IgE functional (V_H-C_ε) and excision circle (C_μ-I_ε) transcripts were almost undetectable in these cells (**Fig. 1a,b**). These results were in contrast to the ability of these B cells to proliferate and produce large amounts of IgM (data not shown and **Fig. 1a**). *AICDA* RNA transcripts were present, indicating that the block in CSR was not a consequence of a defect in the signaling leading to *AICDA* expression (**Fig. 1b**). The possibility of HIGM2 was also excluded, as *AICDA* was unmutated in the three patients (data not shown). IL-4 induction of I_ε-C_ε germline transcription was normal in patient B cells, excluding the possibility of a defect in the CSR initiation step (**Fig. 1b**). Formation of double-stranded DNA breaks (DSBs) in S regions subsequently occurs in the CSR-associated recombination process[14,20,21]. in the CSR-associated recombination process[14,20,21]. After activation by soluble CD40 ligand plus IL-4, B cells from both patients tested (P1 and P3) repeatedly failed to generate DSBs in Sμ regions, in contrast to control B cells, as shown with a ligation-mediated PCR method[21,22]

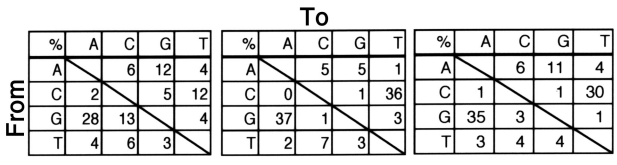

%	Control	P1	P3
Frequency	4.0 (2.6–6.3)	3.4	7.2
Target at dG or dC	63.6 (62–66)	76.8	69.7
Transition at dG or dC	58.9 (57–63)	94.8	93.4
Transversion at dG or dC	41.1 (37–43)	5.2	6.6
Transition at dA or dT	50.4 (33–67)	52.2	49.2
Transversion at dA or dT	49.6 (33–67)	47.8	50.8

Figure 2 SHM frequency and pattern in memory B cells from patients. The frequency and characteristics of SHM in the V_H3-23 region of the IgM were studied in purified $CD19^+CD27^+$ B cells from controls ($n = 7$) and P1 and P3. RT-PCR products amplified by V_H3-23 and C_μ primers amplification were subcloned and sequenced (13 and 10 different clones for P1 and P3, respectively). Bottom, nucleotide changes, shown as percentages. Means and ranges are shown for controls.

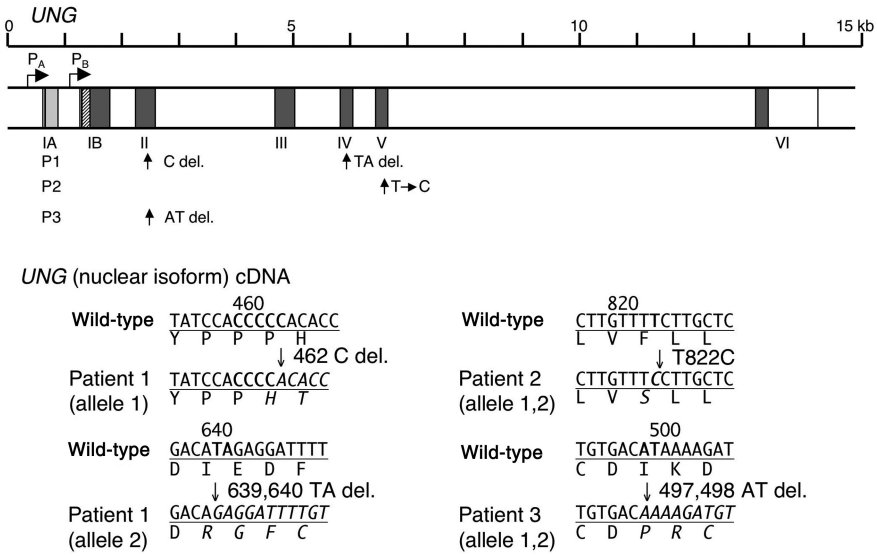

Figure 3 *UNG* mutations in patients. Top, the human *UNG* genomic region. *UNG* has two different promoters (P_B and P_A), leading to two different splice products: the mitochondrial and nuclear isoforms[23]. Below, sequence alterations by mutations and the amino acid changes in the patients (mutation localization on cDNA of nuclear *UNG*). Italics indicate altered nucleotides and amino acids. del., deletion.

(**Fig. 1c**). Thus, as with AID deficiency[14], this HIGM is characterized by defective cleavage of a targeted S region.

Because AID deficiency is also characterized by defective generation of SHM in the V region of immunoglobulin genes, we analyzed SHM in the V_H3-23 region of IgM in purified B ($CD19^+$) memory ($CD27^+$) cell populations from P1 and P3. The ratio of mutated to unmutated clones was within normal range in memory B cells, as was the frequency of mutations per nucleotide (**Fig. 2**). However, the SHM pattern was abnormal, as mutations at dG and dC residues were biased toward transitions (dG→dA, dC→dT), whereas at dA and dT residues, the ratio of transitions toward transversions was similar to control values (**Fig. 2**). Analysis of SHM in P2 B cells was hampered by limited detection of $CD27^+$ peripheral B cells (**Table 1**).

UNG sequence

The HIGM phenotype in these patients resembles the phenotype described as a consequence of homozygous *Ung* inactivation in mice[19], although in the latter a much milder CSR defect was found. We therefore explored the possibility of UNG deficiency in these three patients. As in mice, human *UNG* has two promoters (P_B and P_A) and two alternative splice products: the mitochondrial isoform, which is ubiquitously expressed, and the nuclear isoform, which is strongly expressed in testis, placenta, thymus and other proliferating cells[23,24]. We sequenced genomic DNA encompassing exons I_A (nuclear *UNG*) and I_B-VI. We found deleterious mutations for all three patients (**Fig. 3**). We found two heterozygous mutations in P1, both located in the region encoding the UNG catalytic domain, consisting of a C deletion in exon II and a TA deletion in exon IV. Both lead to the generation of premature stop codons (at codons 141 and 224 of nuclear *UNG*, respectively). The mutation in exon II was inherited from an asymptomatic mother, whereas the mutation in exon IV was inherited from asymptomatic father and was also present in healthy sibling. In P2, we found a homozygous missense mutation in exon V (T→C), which leads to a substitution of a phenylalanine (codon 251 of nuclear *UNG*) with a serine in the catalytic domain of UNG. We found the mutation in one allele in each of the healthy parents. To ensure that the mutation in P2 was not a polymorphism, we sequenced *UNG* from 100 chromosomes, including those from controls from the same ethnic group, and found it was normal. In P3, *UNG* analysis showed a homozygous deletion of two nucleotides (AT) in exon II, leading to the generation of a premature stop codon (at codon 159 of nuclear *UNG*). Thus, in all three patients, these recessive mutations were present in the catalytic domain (codons 84–313 of nuclear *UNG*) shared by the mitochondrial and the nuclear isoforms of *UNG*.

Table 1 Serum immunoglobulin concentrations at diagnosis, and $CD19^+$ and $CD27^+$ cells

	P1	P2	P3	Normal range	
Age at diagnosis (years)	7	3	39	3–8	adult
Serum IgM (mg/dl)	740	267	785	50–118	40–230
IgG (mg/dl)	50	<50	209	680–1260	700–1,600
IgA (mg/dl)	48	25	<7	66–162	70–400
$CD19^+$ (/mm^3)[a]	250	860	138	200–2100	100–500
$CD27^+$ (% of $CD19^+$)[a]	17.0	4.6	17.9	10–20	10–40

[a]P1, P2 and P3 were tested at 26, 6 and 40 years of age, respectively.

UNG expression and function

We established Epstein-Barr virus–immortalized lymphoid cell lines (EBV-LCLs) to study UNG expression and function. We were able to detect mitochondrial *UNG* and nuclear *UNG* RNA transcripts by RT-PCR in EBV-LCLs from controls and patients. We also detected nuclear *UNG* in P2 EBV-LCLs, but this was absent or faintly detectable in P1 and P3 EBV-LCLs, indicating that mutations lead to mRNA instability (**Fig. 4a**). However, immunoprecipitation with an antibody directed to the N-terminal regulatory domain of human UNG (PU1sub) followed by immunoblot analysis with an antibody directed to the C-terminal catalytic domain (PU101) did not detect any material in EBV-LCLs from the three patients (**Fig. 4b**), demonstrating that all mutations lead to protein instability or compromised translation of the mRNA. Correspondingly, we detected no human UNG activity in EBV-LCLs from the patients (**Fig. 4c**), in contrast to results obtained with control EBV-LCLs.

Specific induction of nuclear *UNG* expression during CSR

As UNG was required for CSR, we studied the expression of mitochondrial *UNG* and nuclear *UNG* isoforms in B cells before and after activation by soluble CD40L plus IL-4. Resting and activated $CD19^+$ and $CD19^-$ cells had equal expression of mitochondrial *UNG* transcripts (**Fig. 4d**). In contrast, we only detected nuclear *UNG* transcripts in CSR-induced $CD19^+$ B cells, in correlation with *AICDA* expression (**Fig. 4d**). We were unable to detect nuclear *Ung* transcripts in mouse spleen naive (IgM^+IgD^+) B ($B220^+$) cells. After 5 d of activation by lipopolysaccharide plus IL-4, they were induced similarly to *Aicda* transcripts. In contrast, mitochondrial *Ung* transcripts were expressed in nonactivated as well as activated B cells (**Fig. 4e**).

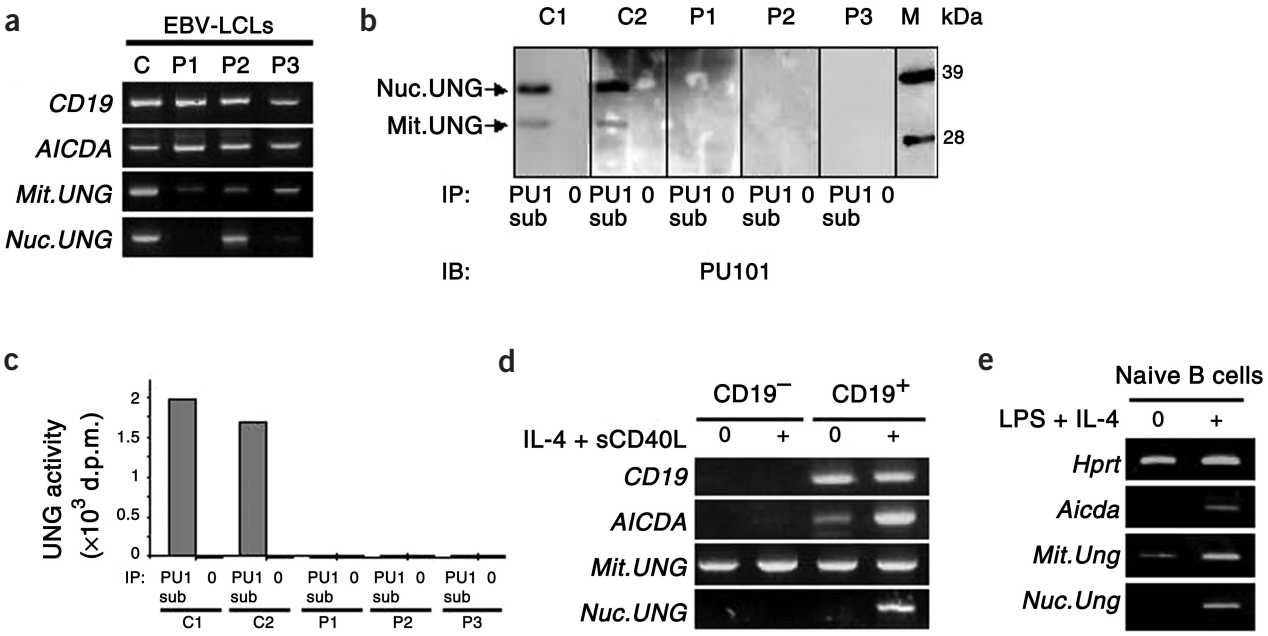

Figure 4 Defective expression and function of UNG in EBV-LCLs of patients. (**a**) *UNG* RNA transcript expression in EBV-LCLs. Mitochondrial and nuclear *UNG* RNA transcript amounts, as detected by RT-PCR, are diminished or absent in P1 (indicating mRNA instability) and normal in P2 and P3. (**b**) UNG protein expression in EBV-LCLs. Immunoblot (IB) of UNG immunoprecipitates from EBV-LCLs fails to demonstrate any mitochondrial or nuclear UNG protein in patients, whereas both forms of UNG are present in the control (C1, C2) cell lines. Identical amounts of total protein were used for immunoprecipitation in all experiments. PU1sub, a non-neutralizing polyclonal antibody directed against the human UNG N-terminal regulatory domain, was used for immunoprecipitation (IP); PU101, a polyclonal antibody against UNG catalytic domain, was used for immunoblot. 0, immunoprecipitation with pre-immune rabbit IgG. M (far right), molecular size markers. (**c**) UNG activity in EBV-LCLs. Specific UNG activity was detected with [^{3}H]dUMP-labeled calf thymus DNA as substrate[47]. UNG activity is present in control EBV-LCLs (C1, C2) after immunoprecipitation with PU1sub. In contrast, there is no activity in EBV-LCLs from patients (P1, P2, P3) or in control beads (0). (**d**) Induction of human nuclear *UNG* in activated control B cells. Transcripts of *CD19*, *AICDA* and *UNG* in control purified CD19$^+$ B cells and CD19$^-$ non-B cells before and after 5 d of *in vitro* activation with soluble CD40L plus IL-4, detected by RT-PCR. Mitochondrial *UNG* is constitutively expressed, whereas nuclear *UNG* is only present in activated CD19$^+$ B cells. (**e**) Induction of mouse nuclear Ung in activated spleen B cells. Mouse spleen naive B cells (B220$^+$IgM$^+$IgD$^+$) were purified and cultured in the presence of lipopolysaccharide (50 μg/ml) plus IL-4 (50 ng/ml) for 5 d. Mitochondrial *Ung* is constitutively expressed, whereas nuclear *Ung* is expressed only in activated B cells. Mit., mitochondrial; Nuc., nuclear.

DISCUSSION

We found UNG deficiency to be linked to a profound inability of human B cells to undergo immunoglobulin CSR associated with qualitative consequences for the pattern of SHM. This recapitulates the UNG-deficient mouse phenotype, although the CSR defect was much more pronounced in humans. Indeed, in mice, the CSR defect is partial *in vivo*, especially found in young mice, whereas it is much more pronounced in *in vitro* experiments[19]. Three possible explanations accounting for this difference can be proposed: other UNGs exert a more redundant activity in mouse B cells; the mismatch-repair enzymes, such as mutS homolog 2 (MSH2) and MSH6, are more important as a surrogate pathway in mice[25,26]; and CSR-deficient mice (such as those deficient in AID, CD40 or CD40L) show a milder phenotype than their human counterparts in terms of serum IgG and IgA isotype concentrations[12,27–29].

As in AID-deficient B cells, the CSR defect in the UNG-deficient B cells seems to occur before S-region cleavage, as evidenced by the lack of DNA breaks. These results strongly support the CSR model in which AID directly deaminates cytosine into uracil residues in the active S regions, followed by uracil removal mediated by UNG, leading to an abasic site. This abasic site can be attacked by an apyrimidinic endonuclease, thus creating a DNA nick[30]. Several groups have concomitantly demonstrated that AID deaminates cytosine in single-stranded DNA but not double-stranded DNA, RNA-DNA hybrids or RNA[16–18]. Transcription of the S region can generate secondary structures such as R-loops, which consist of an RNA-DNA hybrid on the template DNA strand and single-stranded DNA on the nontemplate strand, which may become a target for AID[18,31,32]. It is not known how these DNA breaks on single-stranded DNA result in the DSBs necessary for inter-S-region recombination. AID could exert activity on double-stranded DNA in transcription bubbles[17] or additional, as-yet-unknown factors could be involved[33]. The observation that nuclear *UNG* expression was specifically induced in human and mouse B cells during CSR activation, in parallel with *AICDA* expression, also strengthens, although indirectly, the model described above. In accordance with this model[30], partially defective transversions at dC-dG sites in the SHM process of UNG-deficient B cells would be the consequence of defective error-prone base-excision repair after such site creation at dC residues[30].

Given the sequence similarity to the RNA-editing enzyme APOBEC-1, it has been alternatively proposed that AID edits a putative recombinase-mRNA required for CSR[11]. A protein synthesis–dependent step is downstream from AID activity in CSR, which supports this hypothesis, although this protein synthesis possibly corresponds to the UNG nuclear isoform induction itself[34]. In the RNA-editing hypothesis, UNG might be involved in the base-excision repair process in conjunction with mismatch-repair enzymes, which, when defective, lead to partially impaired CSR and SHM in relevant mouse models[25,26]. Thus, UNG could be part of a complex of proteins, which allows the holding together of cleaved DNA ends[34]; however, this hypothesis does not fit with the defective DSB generation in S regions of UNG-deficient B cells. It is nevertheless possible that

UNG and mismatch-repair enzymes are part of a recombinase complex that mediates additional steps of CSR[34]. There are, however, considerable phenotypic differences in humans between UNG deficiencies and deficiencies in mismatch-repair enzymes, such as mutL homolog 1 (MLH1) and MSH2. Recessive mutations in *MLH1* and *MSH2* predispose to cancer but not to infections[35–38]. Although further studies of CSR status should be done in MLH1- and MSH2-deficient patients, this discrepancy indicates a much more dominant function for UNG in CSR than for mismatch repair enzymes. The profound defect of CSR in UNG-deficient human B cells strongly indicates that other enzymes with UNG activity, including cyclin-like UNG (UNG2)[39,40], single-strand-selective monofunctional UNG 1 (SMUG1)[41], thymine-DNA glycosylase (TDG)[42] and methyl-CpG binding domain protein 4 (MBD4)[43], cannot compensate for UNG deficiency in humans. Moreover, MBD4 deficiency in mice does not impair B cell responses[44]. Although *UNG* mutations in patients have not been directly shown to cause HIGM, the possibility that the nuclear isoform of UNG is involved in CSR is further supported by the observation of its specific induction during *in vitro* B cell activation. In conclusion, the finding that recessive *UNG* mutations are associated with impaired CSR in human B cells and a partially modified pattern of SHM provides further insight into our understanding of the mechanisms underlying secondary immunoglobulin gene alterations in the development of antigen-specific B cell responses.

METHODS

Patients. P1, born to a nonconsanguineous family, presented with recurrent upper and lower respiratory tract infections that had occurred since early childhood. At 7 years of age, the patient was diagnosed with HIGM. A persistent cervical lymph node hyperplasia was noted. The patient is now 27 years old and well on intravenous immunoglobulin (IVIG) treatment. P2, born to a nonconsanguineous family, was diagnosed with HIGM at 3 years of age. The patient is now 6 years old and well controlled on IVIG treatment. P3, born to first-cousin parents, had recurrent upper respiratory tract infections and chronic epididymitis. Cervical and mediastinal lymph node hyperplasia was noted. Antibody titers to pneumococcal and tetanus antigens were found to be decreased, leading to the diagnosis of HIGM when this patient was 39 years of age. The patient is now 40 years old and well on IVIG. All patients have normal T cell counts and functions. Activated T cells had normal expression of CD40L after activation (data not shown). Informed consent was obtained from P1 and P3 and from the parents of P2 for this study, which was approved by the Comité Consultatif de Protection des Personnes participant à une Recherche Biomedicale (Ile de France Paris-Saint-Antoine).

Activation of B cells. Lymphocyte subsets were analyzed as described[45]. Peripheral blood mononuclear cells (PBMCs) were separated by Ficoll-Hypaque density centrifugation (Lymphoprep; Axis-Shield PoC AS). PBMCs were activated *in vitro* with CD32 (FcγRII)-transfected, irradiated L cells (a gift from F. Brière, Schering-Plough) in the presence of anti-CD40 or control IgG (500 ng/ml; Diaclone) or soluble CD40L (500 ng/ml; a gift from Immunex) in combination with IL-4 (100 U/ml; R&D systems) or IL-10 (100 ng/ml, R&D systems). Proliferation was assessed at 5 d by [^{3}H]thymidine uptake. Expression of the genes encoding CD19, AICDA and IgE (GLT, I_ε-C_ε, germline transcripts; CT, C_μ-I_ε, circle transcripts; FT, V_H-C_ε, functional transcripts) was assessed by RT-PCR with the conditions and primers described[10,45] after 5 d of activation with soluble CD40L plus IL-4. *In vitro* production of immunoglobulins (IgM, IgG, IgA and IgE) was assessed by enzyme-linked immunosorbent assay at day 12 in the culture supernatants[45].

Spleen lymphocytes from 6-month-old C57BL/6 mice were isolated by Ficoll-Hypaque gradient centrifugation (NycoPrep 1.077A, Axis-Shield PoC AS). Naive B cells ($B220^+IgM^+IgD^+$) were separated by FACStarPLUS cell sorter (Becton Dickinson) with the following antibodies: biotinylated anti-mouse B220/CD45R (RA3-6B2; BD Pharmingen), fluorescein isothiocyanate (FITC)-conjugated $F(ab')_2$ fragment goat anti-mouse IgM (Jackson ImmunoResearch Laboratories), phycoerythrin (PE)-conjugated rat anti-mouse IgD (Southern Biotechnology Associates) and PE-Cy5-conjugated streptoavidin (BD Pharmingen). Naive B lymphocytes (1×10^6/ml) were activated for 5 d with lipopolysaccharide (50 μg/ml, *Escherichia coli* serotype 026:B6; Sigma) plus recombinant mouse IL-4 (50 ng/ml; R&D Systems).

Detection of DSBs in the Sμ region of the immunoglobulin locus. PBMCs were activated with soluble CD40L plus IL-4. After 5 d of culture, $CD19^+$ B cells were purified by sorting in the presence of propidium iodide to eliminate dead cells. A ligation-mediated PCR method was used to identify DSBs as described[21,22]. Agarose plugs containing genomic DNA (corresponding to 15×10^3 cells/lane) were ligated to a double-stranded linker. Ligated products were amplified by a semi-nested PCR with Sμ-specific and linker primers. PCR products were hybridized with a radiolabeled Sμ probe and detected with phosphorimager FLA3000 (exposure time, 18 h; Fujifilm). T cells activated for 7 d with anti-CD3 plus IL-2 were used as a negative control. Cloning and sequencing of ligation-mediated PCR products from controls were cloned and sequenced as described[21].

Somatic hypermutation in the variable region of IgM. The frequency and characteristics of SHM in the V_H3-23 region of IgM were studied in purified $CD19^+CD27^+$ B cells as described[10]. RT-PCR products of the V_H3-23 region obtained with V_H3-23 and C_μ primers were subcloned and sequenced with the Big Dye DNA sequencing kit (Applied Biosystems) and an automated genetic analyzer (ABI PRISM 377; Applied Biosystems).

Sequence analysis of human *UNG*. Genomic DNA was amplified by PCR with primers directed to intronic or noncoding sequences of *UNG*. PCR products were directly sequenced (primers and conditions for PCR and sequence have been published[46]).

Expression and activity of UNG. *UNG* mRNA transcripts were detected by RT-PCR with primers for mitochondrial *UNG* (36F, 5′-CCGCTCCAGTTTA GAACCTA-3′, and 7Rc, 5′-ACAGCAGCTTCTCAAAGGCC-3′) and nuclear *UNG* (74F, 5′-ATCGGCCAGAAGACGCTCTA-3′, and 7Rc). PCR was completed in 40 cycles (94 °C for 1 min; 62 °C for mitochondrial *UNG* or 65 °C for nuclear *UNG* for 1 min; 72 °C for 2 min). In some experiments, *AICDA* and *UNG* transcripts were tested in sorted $CD19^+$ B cells and $CD19^-$ non-B cells before and after 5 d of activation by soluble CD40L plus IL-4.

Mouse *Ung* mRNA transcripts were detected by RT-PCR with primers for mouse mitochondrial *Ung* (45F, 5′-CGGCGGTCTTTGCGGTTG-3′, and UngR, 5′-GACAACCTTCACATCTCG-3′) and mouse nuclear *Ung* (72F, 5′-ATCGGCCAGAAGACCCTATA-3′, and mUng/exIVR, 5′-CCCACCCTGAC AAATCCCCA-3′). PCR was completed in 40 cycles (94 °C for 1 min; 52 °C for 1 min; 72 °C for 2 min). Transcripts of mouse *Aicda* and *Hprt* (hypoxanthine guanine phosphoribosyl transferase) were detected as described[12].

For analysis of UNG protein, cell-free extracts from EBV-LCLs were immunoprecipitated with magnetic protein A Dynabeads (Dynal) covalently attached to a non-neutralizing polyclonal antibody (PU1sub) directed against the entire human nuclear isoform of UNG and part of the human mitochondrial UNG N-terminal regulatory sequence. Control beads were labeled with the same amount of preimmune IgG from the same rabbit. After polyacrylamide electrophoresis of the eluted immunoprecipitates and electrotransfer to PVDF membranes (Immobilon; Millipore), UNG proteins were detected with a primary polyclonal antibody (PU101) directed against the UNG catalytic domain[47] and secondary horseradish peroxidase–labeled swine anti-rabbit IgG (DakoCytomation) and finally with SuperSignal West femto (Pierce Biotechnology), and were visualized in a Kodak 2000R Image station (Eastman Kodak Company). For specific analysis of UNG activity, cell free extracts from EBV-LCLs of controls and patients were incubated with PU1sub polyclonal antibody or preimmue IgG-labeled beads. After thorough washing, the beads were analyzed for UNG activity by measurement of the released uracil from the assay buffer containing [^{3}H]dUMP-labeled calf thymus DNA substrate[47].

UniGene accession numbers. Human *UNG*, Hs.78853; human mitochondrial *UNG*, NM_003362; human nuclear *UNG*, NM_080911; mouse mitochondrial *Ung*, X99018; mouse nuclear *Ung*, Y08975.

ACKNOWLEDGMENTS

We thank O. Hermine (Paris, France) and M. Endou (Iwate, Japan) for referral of patients. This work was supported by grants from Institut National de la Santé et de la Recherche Médicale, Association pour la Recherche sur le Cancer, la Ligue Contre le Cancer, the European Economic Community (contract QLG1-CT-2001-01536- IMPAD), the Research Council of Norway, the Norwegian Cancer Association, the Svanhild and Arne Must Fund for Medical Research and the Louis Jeantet Foundation, and by grants from the National Institutes of Health (HD 17427-33), the March of Dimes Birth Defects Foundation (96-0330), the Immunodeficiency Foundation and the Jeffrey-Modell Foundation. P.R. is a scientist from Centre National de la Recherche Scientifique (Paris, France). N.C. is supported by the Association pour la Recherche sur le Cancer.

COMPETING INTERESTS STATEMENT

The authors declare that they have no competing financial interests.

Received 19 May; accepted 23 July 2003
Published online at http://www.nature.com/natureimmunology/

1. Manis, J.P., Tian, M. & Alt, F.W. Mechanism and control of class-switch recombination. *Trends Immunol.* **23**, 31–39 (2002).
2. Honjo, T., Kinoshita, K. & Muramatsu, M. Molecular mechanism of class switch recombination: linkage with somatic hypermutation. *Annu. Rev. Immunol.* **20**, 165–196 (2002).
3. Kinoshita, K. & Honjo, T. Linking class-switch recombination with somatic hypermutation. *Nat. Rev. Mol. Cell Biol.* **2**, 493–503 (2001).
4. Durandy, A. Hyper-IgM syndromes: a model for studying the regulation of class switch recombination and somatic hypermutation generation. *Biochem. Soc. Trans.* **30**, 815–818 (2002).
5. Korthauer, U. *et al.* Defective expression of T-cell CD40 ligand causes X-linked immunodeficiency with hyper-IgM. *Nature* **361**, 539–541 (1993).
6. DiSanto, J.P., Bonnefoy, J.Y., Gauchat, J.F., Fischer, A. & de Saint Basile, G. CD40 ligand mutations in X-linked immunodeficiency with hyper-IgM. *Nature* **361**, 541–543 (1993).
7. Aruffo, A. *et al.* The CD40 ligand, gp39, is defective in activated T cells from patients with X-linked hyper-IgM syndrome. *Cell* **72**, 291–300 (1993).
8. Allen, R.C. *et al.* CD40 ligand gene defects responsible for X-linked hyper-IgM syndrome. *Science* **259**, 990–993 (1993).
9. Ferrari, S. *et al.* Mutations of CD40 gene cause an autosomal recessive form of immunodeficiency with hyper IgM. *Proc. Natl. Acad. Sci. USA* **98**, 12614–12619 (2001).
10. Revy, P. *et al.* Activation-induced cytidine deaminase (AID) deficiency causes the autosomal recessive form of the Hyper-IgM syndrome (HIGM2). *Cell* **102**, 565–575 (2000).
11. Muramatsu, M. *et al.* Specific expression of activation-induced cytidine deaminase (AID), a novel member of the RNA-editing deaminase family in germinal center B cells. *J. Biol. Chem.* **274**, 18470–18476 (1999).
12. Muramatsu, M. *et al.* Class switch recombination and hypermutation require activation-induced cytidine deaminase (AID), a potential RNA editing enzyme. *Cell* **102**, 553–563 (2000).
13. Bross, L., Muramatsu, M., Kinoshita, K., Honjo, T. & Jacobs, H. DNA double-strand breaks: prior to but not sufficient in targeting hypermutation. *J. Exp. Med.* **195**, 1187–1192 (2002).
14. Petersen, S. *et al.* AID is required to initiate Nbs1/g-H2AX focus formation and mutations at sites of class switching. *Nature* **414**, 660–665 (2001).
15. Petersen-Mahrt, S.K., Harris, R.S. & Neuberger, M.S. AID mutates *E. coli* suggesting a DNA deamination mechanism for antibody diversification. *Nature* **418**, 99–104 (2002).
16. Chaudhuri, J. *et al.* Transcription-targeted DNA deamination by the AID antibody diversification enzyme. *Nature* **422**, 726–730 (2003).
17. Bransteitter, R., Pham, P., Scharff, M.D. & Goodman, M.F. Activation-induced cytidine deaminase deaminates deoxycytidine on single-stranded DNA but requires the action of RNase. *Proc. Natl. Acad. Sci. USA* **100**, 4102–4107 (2003).
18. Ramiro, A.R., Stavropoulos, P., Jankovic, M. & Nussenzweig, M.C. Transcription enhances AID-mediated cytidine deamination by exposing single-stranded DNA on the nontemplate strand. *Nat. Immunol.* **4**, 452–456 (2003).
19. Rada, C. *et al.* Immunoglobulin isotype switching is inhibited and somatic hypermutation perturbed in UNG-deficient mice. *Curr. Biol.* **12**, 1748–1755 (2002).
20. Wuerffel, R.A., Du, J., Thompson, R.J. & Kenter, A.L. Ig Sg3 DNA-specific double strand breaks are induced in mitogen-activated B cells and are implicated in switch recombination. *J. Immunol.* **159**, 4139–4144 (1997).
21. Imai, K. *et al.* Hyper-IgM syndrome type 4 with a B lymphocyte-intrinsic selective deficiency in Ig class-switch recombination. *J. Clin. Invest.* **112**, 136–142 (2003).
22. Papavasiliou, F.N. & Schatz, D.G. Cell-cycle-regulated DNA double-stranded breaks in somatic hypermutation of immunoglobulin genes. *Nature* **408**, 216–221 (2000).
23. Nilsen, H. *et al.* Nuclear and mitochondrial uracil-DNA glycosylases are generated by alternative splicing and transcription from different positions in the UNG gene. *Nucleic Acids Res.* **25**, 750–755 (1997).
24. Otterlei, M. *et al.* Nuclear and mitochondrial splice forms of human uracil-DNA glycosylase contain a complex nuclear localisation signal and a strong classical mitochondrial localisation signal, respectively. *Nucleic Acids Res.* **26**, 4611–4617 (1998).
25. Ehrenstein, M.R. & Neuberger, M.S. Deficiency in Msh2 affects the efficiency and local sequence specificity of immunoglobulin class-switch recombination: parallels with somatic hypermutation. *EMBO J.* **18**, 3484–3490 (1999).
26. Schrader, C.E., Edelmann, W., Kucherlapati, R. & Stavnezer, J. Reduced isotype switching in splenic B cells from mice deficient in mismatch repair enzymes. *J. Exp. Med.* **190**, 323–330 (1999).
27. Castigli, E. *et al.* CD40-deficient mice generated by recombination-activating gene-2-deficient blastocyst complementation. *Proc. Natl. Acad. Sci. USA* **91**, 12135–12139 (1994).
28. Xu, J. *et al.* Mice deficient for the CD40 ligand. *Immunity* **1**, 423–431 (1994).
29. Kawabe, T. *et al.* The immune responses in CD40-deficient mice: impaired immunoglobulin class switching and germinal center formation. *Immunity* **1**, 167–178 (1994).
30. Di Noia, J. & Neuberger, M.S. Altering the pathway of immunoglobulin hypermutation by inhibiting uracil-DNA glycosylase. *Nature* **419**, 43–48 (2002).
31. Yu, K., Chedin, F., Hsieh, C.L., Wilson, T.E. & Lieber, M.R. R-loops at immunoglobulin class switch regions in the chromosomes of stimulated B cells. *Nat. Immunol.* **4**, 442–451 (2003).
32. Shinkura, R. *et al.* The influence of transcriptional orientation on endogenous switch region function. *Nat. Immunol.* **4**, 435–441 (2003).
33. Fugmann, S.D. & Schatz, D.G. RNA AIDs DNA. *Nat. Immunol.* **4**, 429–430 (2003).
34. Doi, T., Kinoshita, K., Ikegawa, M., Muramatsu, M. & Honjo, T. *De novo* protein synthesis is required for the activation-induced cytidine deaminase function in class-switch recombination. *Proc. Natl. Acad. Sci. USA* **100**, 2634–2638 (2003).
35. Vilkki, S. *et al.* Extensive somatic microsatellite mutations in normal human tissue. *Cancer Res.* **61**, 4541–4544 (2001).
36. Wang, Q. *et al.* Neurofibromatosis and early onset of cancers in hMLH1-deficient children. *Cancer Res.* **59**, 294–297 (1999).
37. Whiteside, D. *et al.* A homozygous germ-line mutation in the human MSH2 gene predisposes to hematological malignancy and multiple cafe-au-lait spots. *Cancer Res.* **62**, 359–362 (2002).
38. Bougeard, G. *et al.* Early onset brain tumor and lymphoma in MSH2-deficient children. *Am. J. Hum. Genet.* **72**, 213–216 (2003).
39. Muller, S.J. & Caradonna, S. Isolation and characterization of a human cDNA encoding uracil-DNA glycosylase. *Biochim. Biophys. Acta* **1088**, 197–207 (1991).
40. Muller, S.J. & Caradonna, S. Cell cycle regulation of a human cyclin-like gene encoding uracil-DNA glycosylase. *J. Biol. Chem.* **268**, 1310–1319 (1993).
41. Nilsen, H. *et al.* Excision of deaminated cytosine from the vertebrate genome: role of the SMUG1 uracil-DNA glycosylase. *EMBO J.* **20**, 4278–4286 (2001).
42. Neddermann, P. *et al.* Cloning and expression of human G/T mismatch-specific thymine-DNA glycosylase. *J. Biol. Chem.* **271**, 12767–12774 (1996).
43. Hendrich, B., Hardeland, U., Ng, H.H., Jiricny, J. & Bird, A. The thymine glycosylase MBD4 can bind to the product of deamination at methylated CpG sites. *Nature* **401**, 301–304 (1999).
44. Bardwell, P.D. *et al.* Cutting edge: the G-U mismatch glycosylase methyl-CpG binding domain 4 is dispensable for somatic hypermutation and class switch recombination. *J. Immunol.* **170**, 1620–1624 (2003).
45. Durandy, A. *et al.* Abnormal CD40-mediated activation pathway in B lymphocytes from patients with hyper-IgM syndrome and normal CD40 ligand expression. *J. Immunol.* **158**, 2576–2584 (1997).
46. Kvaloy, K. *et al.* Sequence variation in the human uracil-DNA glycosylase (UNG) gene. *Mutat. Res.* **461**, 325–338 (2001).
47. Slupphaug, G. *et al.* Properties of a recombinant human uracil-DNA glycosylase from the UNG gene and evidence that UNG encodes the major uracil-DNA glycosylase. *Biochemistry* **34**, 128–138 (1995).